Beam Steering for the Misalignment in UCA-Based OAM Communication Systems

Rui Chen, *Member, IEEE,* Hui Xu, Marco Moretti, *Member, IEEE* and Jiandong Li, *Senior Member, IEEE*

***Abstract*—Radio frequency orbital angular momentum (RF OAM) is a technique that provides extra degrees of freedom to improve spectrum efficiency of wireless communications. However, OAM requires perfect alignment of the transmit and the receive antennas and this harsh precondition greatly challenges practical RF OAM applications. In this paper, we first investigate the effect of the non-parallel misalignment on the channel capacity of an OAM communication system equipped with the uniform circular array (UCA) and then propose a transmit/receive beam steering approach to circumvent the large performance degradation in not only the non-parallel case but also the off-axis and other general misalignment cases. The effectiveness of the beam steering approach is validated through both mathematical analysis and numerical simulations.**

***Index Terms*—Orbital angular momentum (OAM), uniform circular array (UCA), misalignment, beam steering**

I. Introduction

The explosive growth of multimedia services and the advent of new wireless paradigms such as Internet of Things (IoT) calls for a large increase of wireless data capacity. On the other hand, the radio frequency (RF) spectrum is limited and the available spectral resources can not accommodate all the requests for higher data rates. To deal with this problem, research has explored innovative techniques and concepts such as advanced modulation and coding schemes, cognitive radio and multiple-input multiple-output (MIMO). Since the discovery in 1992 that light beams with helical phase fronts can carry orbital angular momentum (OAM) [1], a great research effort has been focused on OAM at RF as a novel approach for multiplexing a set of orthogonal modes on the same frequency channel and achieve high spectral efficiencies.

Recent experiments have shown that optical OAM can produce dramatic increases in capacity and spectral efficiency: in [2], for example, polarization-multiplexed data streams travelling along a beam of light with 8 different OAM modes can reach a rate up to 2.5 Tbits (equivalent to 66 DVDs) per second. In the same time, the famous ‘Venice experiment’ [3] has shown that OAM can be succesfully applied to RF transmissions as first claimed in [4]. Since then, RF OAM communications has attracted a lot of attention [5]–[12]. The work in [5] shows that it is possible to achieve 32Gbit/s in a wireless communication link at 28 GHz by multiplexing 8 OAM channels generated by spiral phase plates (SPPs). To overcome the complexity of using SPP, [6], [13] and [14] have verified in theory and in practice the feasibility of employing uniform circular array (UCA) to generate OAM waves .

Rui Chen, Hui Xu and Jiandong Li are with the State Key Laboratory of Integrated Service Networks (ISN), Xidian University, Shaanxi 710071, China (e-mail: rchen@xidian.edu.cn).

M. Moretti is with the University of Pisa, Dipartimento di Ingegneria dell'Informazione, Italy (e-mail: marco.moretti@iet.unipi.it).

One of the main obstacles for the commercial deployment of RF-OAM systems is the severe precondition that the transmit and receive antenna arrays need perfect alignment. If the precondition is not accurately met, the system performance quickly deteriorates. The authors in [7] summarize the effects of misalignment qualitatively through simulations and experiments on the SPP-based OAM system in millimeter wave band. The performance degradation caused by non-parallel misalignment in the UCA-based OAM system is shown in [8] through electromagnetic simulation. Nevertheless, to the best of our knowledge, the quantitative analysis of the misalignment effects in the UCA-based OAM system has not been performed yet.

In this paper we investigate the effect of misalignment between the transmit and the receive UCA in a RF OAM communication system and prove that beam steering is an effective way to improve the system performance in case of misalignment. In detail, we first derive the channel model of the basic non-parallel misalignment case. Then, we analyze the effect of oblique angle on the OAM channel capacity. At last, we propose an OAM beam steering method to circumvent the large performance degradation due to the non-parallel case, the off-axis and other general cases. Mathematical analysis and numerical results validated our proposed method.

Notation: Upper (lower) case boldface letters are for matrices (vectors); $(\cdot)^H$ denotes complex conjugate transpose (Hermitian), $(\cdot)^T$ denotes transpose, $|\cdot|$ denotes modulus of a complex number and $\odot$ denotes Hadamard product.

II. System Model

We consider a RF OAM communication system, where the OAM beam is generated by an N-elements UCA at the transmitter and received by another N-elements UCA at the receiver. In practice, the perfect alignment between the transmit UCA and the receive UCA may not be easy to realize. Thus, the two common misalignment cases: non-parallel and off-axis could be observed [7], [9]. Following the analysis in Section IV, the off-axis case could be decomposed into two non-parallel cases and, accordingly, we only delve into the basic non-parallel case as shown in Fig.1.

A. Channel Model

In free space communications, propagation through the RF channel leads to attenuation and phase rotation of the transmitted signal. This effect is modelled by the multiplication for

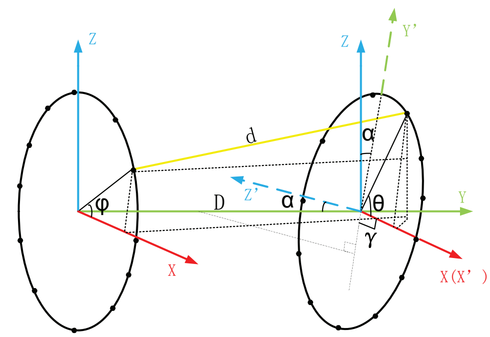

Fig. 1: The geometrical model of the transmit and the receive UCA in the non-parallel misalignment case.

a complex constant h, whose value depends on the distance d between the transmit and receive antenna [15]:

$$h(d) = \beta \frac{\lambda}{4\pi d} \exp\left(-j\frac{2\pi d}{\lambda}\right), \tag{1}$$

where λ is the wavelength, and $\lambda/4\pi d$ denotes the degradation of amplitude, and the complex exponential term is the phase difference due to the propagation distance. The term β models all constants relative to the antenna elements and their patterns.

Let us assume that the number of the transmit and receive antenna elements is equal to N. Thus, according to (1) and the geometric relationship depicted in Fig.1, the channel coefficients from the n-th ($1 \leq n \leq N$) transmit antenna element to the m-th ($1 \leq m \leq N$) receive antenna element can be expressed as $h_{m,n} = h(d_{m,n})$, where the transmission distance $d_{m,n}$ is calculated as

$$\begin{aligned} d_{m,n} = \big[& R_r^2 + R_t^2 + D^2 + 2DR_r \sin\theta \sin\alpha \\ & - 2R_r R_t \left(\cos\varphi\cos\theta + \sin\varphi\sin\theta\cos\alpha\right)\big]^{1/2}, \end{aligned} \tag{2}$$

where D is the distance between the transmit and the receive UCA centers, R_t and R_r are respectively the radiuses of the transmit and the receive UCAs, $\varphi = [2\pi(n-1)/N + \varphi_0]$ and $\theta = [2\pi(m-1)/N + \theta_0]$ are respectively the azimuthal angles of the transmit and the receive UCAs, φ_0 and θ_0 are the corresponding initial angles of the first reference antenna element in both UCA, α is the oblique angle shown in Fig.1.

In the end, the channel matrix of the UCA-based free space OAM communication system can be expressed as $\mathbf{H} = [h(d_{m,n})]_{N\times N}$. When $\alpha = 0$, $\mathbf{H}$ is a circulant matrix that can be decomposed by N-dimentional Fourier matrix $\mathbf{F}_N$ as $\mathbf{H} = \mathbf{F}_N^H \mathbf{\Lambda} \mathbf{F}_N$, $\mathbf{\Lambda}$ is a diagonal matrix with the eigenvalues of $\mathbf{H}$ on its diagonal.

B. UCA-Based OAM Communication System

The OAM beam is generated by the UCA by feeding the antenna elements with the same input signal, but with a successive phase shift from element to element. Thus, after a full turn the phase has the increment of $2\pi\ell$, where ℓ is an unbounded integer termed as OAM mode number [1].

Thus, generating the OAM beam with the mode number ℓ could be formulated as

$$\mathbf{x}_t = \frac{1}{\sqrt{N}} \sum_{n=1}^{N} x(\ell) \exp\left(j\ell\frac{2\pi(n-1)}{N}\right) = \mathbf{f}^H(\ell) x(\ell), \tag{3}$$

where $x(\ell)$ is the information signal to be transmitted by ℓ-mode beam, $\mathbf{x}_t$ is the generated vortex signal vector, $\mathbf{f}(\ell) = \frac{1}{\sqrt{N}}[1, T^{\ell}, \cdots, T^{\ell(N-1)}]$, $T = \exp(-j\frac{2\pi}{N})$. Accordingly, receiving the OAM beam with the mode number ℓ' could be formulated as

$$y(\ell') = \frac{1}{\sqrt{N}} \sum_{m=1}^{N} y_{r,m} \exp\left(-j\ell'\frac{2\pi(m-1)}{N}\right) = \mathbf{f}(\ell')\mathbf{y}_r, \tag{4}$$

where $\mathbf{y}_r = [y_{r,1}, y_{r,2}, \cdots, y_{r,N}]^T$ is the received vortex signal vector, and $y(\ell')$ is the ℓ'-mode OAM despiralized information signal. Then, the orthogonality between OAM modes could be revealed by

$$y(\ell') = \mathbf{f}(\ell')\mathbf{f}^H(\ell)x(\ell) = \begin{cases} x(\ell) & \ell' = \ell \\ 0 & \ell' \neq \ell. \end{cases} \tag{5}$$

Therefore, the transmission of N modes-multiplexed OAM beams in the free space channel $\mathbf{H}$ drives the despiralized information signal vector $\mathbf{y}$ to take the form

$$\mathbf{y} = \mathbf{F}_N \left(\mathbf{H}\mathbf{F}_N^H \mathbf{x} + \mathbf{n}\right), \tag{6}$$

where $\mathbf{y} = [y(1), y(2), \cdots, y(N)]^T$, $\mathbf{x} = [x(1), x(2), \cdots, x(N)]^T$, $\mathbf{F}_N = [\mathbf{f}^H(1), \mathbf{2}^H(\ell), \cdots, \mathbf{f}^H(N)]^H$ is Fourier matrix, and $\mathbf{n}$ is the complex Gaussian noise vector with zero mean and covariance matrix $\sigma_n^2 \mathbf{I}_N$. In the case of perfect alignment, with the circulant matrix decomposition, (6) could be further simplified as [15]

$$\mathbf{y} = \mathbf{\Lambda}\mathbf{x} + \tilde{\mathbf{n}}, \tag{7}$$

where $\tilde{\mathbf{n}} = \mathbf{F}_N \mathbf{n}$. The equation (7) shows that there is not any inter-mode interference at the receiver. Thus, in contrast to MIMO system, OAM system doesn't need complex equalization with the channel information [10]. However, once the perfect alignment is not met, the decomposition of $\mathbf{H}$ doesn't hold, which results in the inter-mode interference at the receiver and thus poor system performance. Moreover, we find that the performance of the single-mode OAM system degrades severely even if α has a small value. Therefore, to isolate the impact of inter-mode interference while simplifying the analysis, we consider the OAM system with only one single mode in this paper.

For the transmission of the ℓ-mode OAM beam, the despiralized information signal $y(\ell)$ can be written as

$$y(\ell) = \mathbf{f}(\ell)\left(\mathbf{H}\mathbf{f}^H(\ell)x + \mathbf{n}\right) = h_{\text{eff}}^N(\ell)x + \tilde{n}, \tag{8}$$

where $h_{\text{eff}}^N(\ell) = \mathbf{f}(\ell)\mathbf{H}\mathbf{f}^H(\ell)$ is the ℓ-mode effective OAM channel. Since $\mathbf{f}(\ell)$ doesn't change the noise energy, $\tilde{n}$ is also complex Gaussian variable with zero mean and variance σ_n^2. Thus, the channel capacity of the ℓ-mode OAM communication system described in (8) can be formulated as

$$C_N(\ell) = \log_2\left(1 + \frac{P_\ell |h_{\text{eff}}^N(\ell)|^2}{\sigma_n^2}\right) \quad \text{bit/sec/Hz}, \tag{9}$$

where P_ℓ is the transmit power of the ℓ-mode OAM beam.

III. The Effect of Oblique Angle on Channel Capacity

If the transmitter and receiver are aligned i.e. $\alpha = 0$, the channel matrix $\mathbf{H}$ is a circulant matrix that can be decomposed into a diagonal matrix by one DFT matrix and one inverse DFT (IDFT) matrix. Thus, the effective channel gain is equal to the modulus of the ℓth eigenvalue of $\mathbf{H}$, which is similar to the eigenmode transmission in MIMO systems. However, once $\alpha \neq 0$, the circulant property of $\mathbf{H}$ does not hold any longer. As a result, the OAM channel capacity deteriorates and becomes worse than MIMO channel capacity. Therefore, it is necessary to figure out the effect of oblique angle α on the OAM channel capacity.

Assuming that the transmit and the receive UCAs are placed in the far-field distance of each other [16], i.e. $D \gg R_t$ and $D \gg R_r$, thus we can approximate $d_{m,n}$ in (2) as

$$\begin{aligned} d_{m,n} \overset{(a)}{\approx} & \sqrt{R_r^2 + R_t^2 + D^2} - \frac{R_r R_t \cos\varphi \cos\theta}{\sqrt{R_r^2 + R_t^2 + D^2}} \\ & - \frac{R_r R_t \sin\varphi \sin\theta \cos\alpha - D R_r \sin\theta \sin\alpha}{\sqrt{R_r^2 + R_t^2 + D^2}} \\ \overset{(b)}{\approx} & D - \frac{R_r R_t}{D} \cos\varphi \cos\theta - \frac{R_r R_t}{D} \sin\varphi \sin\theta \cos\alpha \\ & + R_r \sin\theta \sin\alpha, \end{aligned} \tag{10}$$

where (a) uses the method of completing the square and the condition $D \gg R_t, R_r$ as same as the simple case $\sqrt{a^2 - 2b} \approx a - \frac{b}{a}, a \gg b$; (b) is directly obtained from the condition $D \gg R_t, R_r$. Then, substituting (10) into (1) and abbreviating $h(d_{m,n})$ to $h_{m,n}$, we thus have

$$\begin{aligned} h_{m,n} \overset{(c)}{\approx} & \beta \frac{\lambda}{4\pi D} \exp\Bigg(- j\frac{2\pi}{\lambda} D + j\frac{2\pi R_r R_t}{\lambda D} \cos\varphi \cos\theta \\ & + j\frac{2\pi R_r R_t}{\lambda D} + \sin\varphi \sin\theta \cos\alpha - j\frac{2\pi R_r}{\lambda} \sin\theta \sin\alpha \Bigg), \end{aligned} \tag{11}$$

where (c) neglects a few minor terms in the denominator of the amplitude term and thus only $4\pi D$ is left. Having (11), the modulus of the ℓ-mode effective OAM channel $h_{\text{eff}}^N(\ell)$ is derived as

$$\begin{aligned} & |h_{\text{eff}}^N(\ell)| = |\mathbf{f}(\ell) \mathbf{H} \mathbf{f}^H(\ell)| \\ & = \frac{1}{N} \left| \sum_{n=1}^{N} \sum_{m=1}^{N} h_{m,n} \exp\left(-j\frac{2\pi(m-1)l}{N} + j\frac{2\pi(n-1)l}{N} \right) \right| \\ & \approx \frac{1}{N} \Bigg| \sum_{n=1}^{N} \sum_{m=1}^{N} \beta \frac{\lambda}{4\pi D} \exp\Bigg(j\frac{2\pi R_r R_t}{\lambda D} \cos\frac{2\pi(n-m)}{N} \\ & \qquad - j\frac{2\pi D}{\lambda} - j\frac{2\pi R_r \alpha}{\lambda} \sin\frac{2\pi(m-1)}{N} + j\frac{2\pi(n-m)l}{N} \Bigg) \Bigg| \\ & \overset{q=n-m}{=} \eta \left| \sum_{q=0}^{N-1} \exp\left(j\frac{2\pi R_r R_t}{\lambda D} \cos\frac{2\pi q}{N} + j\frac{2\pi q l}{N} \right) \right| \\ & \qquad \cdot \left| \sum_{m=1}^{N} \exp\left(-j\frac{2\pi R_r \alpha}{\lambda} \sin\frac{2\pi(m-1)}{N} \right) \right|, \end{aligned} \tag{12}$$

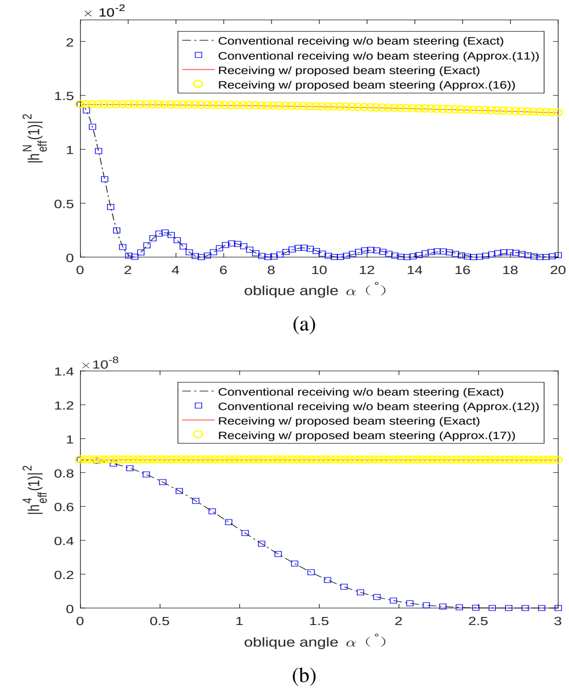

Fig. 2: The modulus squared of the effective OAM channel vs. oblique angle (a) large-scale UCAs; (b) 4-elements UCAs.

where $\eta = \frac{\beta\lambda}{4\pi D N}$. It is obvious to see from (12) that α is only included in the second summation term, and if $\alpha = 0$ all the powers in the sum become 1 so that the sum achieves its maximum value N. Otherwise, the modulus value of the second summation term and thus the value of $|h_{\text{eff}}^N(\ell)|$ decreases rapidly even if α has a small value. The phenomenon is easy to understand, because in the addition the N position vectors with different arguments in the complex plane almost cancel each other out when $\alpha > \frac{\lambda}{R_r}$.

Let us examine the simple parameters $N = 4$ and $\ell = 1$, which are the same as the setting of the experimental system in [6]. Then, $|h_{\text{eff}}^4(1)|^2$ could be expressed as

$$\begin{aligned} |h_{\text{eff}}^4(1)|^2 \approx & \frac{\lambda^2}{16\pi^2 D^2} \Bigg(\sin\frac{2\pi R_r R_t}{\lambda D} \\ & + \cos\frac{2\pi R_r \sin\alpha}{\lambda} \sin\frac{2\pi R_r R_t \cos\alpha}{\lambda D} \Bigg)^2. \end{aligned} \tag{13}$$

Thus, when α goes to zero, (13) could be further approximated by the Taylor series expansion $\sin\alpha \approx \alpha$ and $\cos\alpha \approx 1 - \frac{\alpha^2}{2}$, and finally takes the form

$$|h_{\text{eff}}^4(1)|^2 \approx \frac{\lambda^2}{16\pi^2 D^2} \sin^2\frac{2\pi R_r R_t}{\lambda D} \left(1 + \cos\frac{2\pi R_r \alpha}{\lambda} \right)^2. \tag{14}$$

The (14) indicates that the value of $|h_{\text{eff}}^4(1)|^2$ will fall from its maximum at $\alpha = 0$ to zero at $\alpha = \frac{\lambda}{2R_r}$. Since in general λ is much smaller than R_r, the effective channel gain and thus the OAM channel capacity drops rapidly as long as α is comparable to $\frac{\lambda}{2R_r}$. We also illustrate the effect of oblique angle on the effective channel gain with $R_r = 10\lambda$, $D = 1000\lambda$, the large-scale UCAs ($N = 5000$) in Fig.2(a) and the

4-elements UCAs in Fig.2(b). The numerical results show that the rapid decline occurs once α is beyond about 2 degrees.

IV. Proposed Beam Steering for the Misaligned UCA-Based OAM Systems

To alleviate the performance degradation induced by the misalignment, we propose applying the beam steering to the UCA-based OAM communication systems, which is based on the feasibility of tuning the angle of an OAM beam [12]. We first deliberate on the beam steering in the non-parallel case and then extend it to the off-axis and the general cases.

A. Non-parallel Case

For the non-parallel case as shown in Fig.3, the beam steering approach is to compensate the changed phases caused by oblique angle at the phase shifters of the receive UCA, given that the direction of arrival (DOA) of the OAM beam is perfectly estimated. Specifically, all the phase shifters can be adjusted from the normal phases used for despiralization only to the new phases used for both despiralization and beam steering towards the DOA.

To develop the new phases, we reestablish the coordinate system X'Y'Z' with its origin located in the center of the receive UCA as shown in Fig.1. Then, the azimuth and the elevation angle of the incident OAM beam are respectively $-\pi/2$ and α. Through calculating the phase difference between the reference element and the mth element of the receive UCA, the receive beam steering vector $\mathbf{a}$ could be written as $\mathbf{a} = [1, e^{-jW_2}, \cdots, e^{-jW_N}]$, where

$$W_m = \frac{2\pi R_r}{\lambda} \cos\left(\frac{2\pi(m-1)}{N} + \frac{\pi}{2}\right) \sin\alpha, \qquad (15)$$

$m = 1, \cdots, N$. After involving these phases into the original phases in $\mathbf{f}(\ell)$ at the phase shifters of the receive UCA, the ℓ-mode effective OAM channel becomes

$$h'^{N}_{\text{eff}}(\ell) = \big(\mathbf{f}(\ell) \odot \mathbf{a}\big)\mathbf{H}\mathbf{f}^H(\ell). \qquad (16)$$

Thus, the modulus of the ℓ-mode effective OAM channel could be written as

$$\begin{aligned} |h'^{N}_{\text{eff}}(\ell)| \approx \eta \Bigg| \sum_{m=1}^{N}\sum_{n=1}^{N} \exp\bigg(& j\frac{2\pi(n-1)l}{N} - j\frac{2\pi(m-1)l}{N} \\ & + j\frac{2\pi R_r R_t}{\lambda D}\cos\frac{2\pi(n-1)}{N}\cos\frac{2\pi(m-1)}{N} - j\frac{2\pi D}{\lambda} \\ & + j\frac{2\pi R_r R_t}{\lambda D}\sin\frac{2\pi(n-1)}{N}\sin\frac{2\pi(m-1)}{N}\cos\alpha\bigg)\Bigg| \\ \overset{(d)}{\approx} \eta \Bigg| \sum_{m=1}^{N}\sum_{q=0}^{N-1} & \exp\left(j\frac{2\pi R_r R_t}{\lambda D}\cos\frac{2\pi q}{N} + j\frac{2\pi q l}{N}\right) \\ \cdot \exp & \left(-j\frac{\alpha^2 \pi R_r R_t}{\lambda D}\sin\frac{2\pi(q+m-1)}{N}\sin\frac{2\pi(m-1)}{N}\right)\Bigg|, \end{aligned} \qquad (17)$$

where (d) applies the substitution $q = n - m$ and the approximation $\cos\alpha \approx 1 - \frac{\alpha^2}{2}$ with the focus on the small values of α. Comparing (17) with (12), we find that in (17), D appears in the denominator of the term containing α. Thus, the effect of α is discounted greatly by D that is much larger than R_t, R_r and α. It follows that the value of $|h'^{N}_{\text{eff}}(\ell)|$ is not sensitive to the oblique angle α.

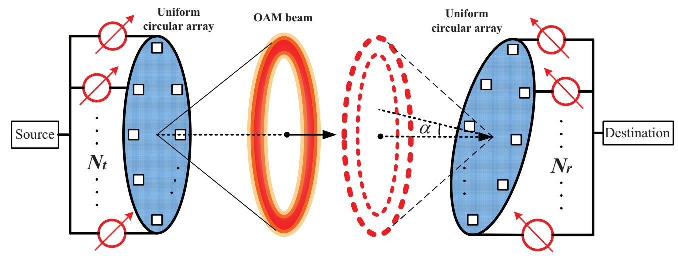

Fig. 3: The diagram of the receive beam steering in the off-axis misalignment case.

Corresponding to (13), we also examine the simple case that $N = 4$ and $\ell = 1$. The modulus squared of the effective OAM channel with the receive beam steering can be expressed as

$$|h'^{4}_{\text{eff}}(1)|^2 \approx \frac{\lambda^2}{4\pi^2 D^2}\left(\sin\frac{2\pi R_r R_t}{\lambda D} + \sin\frac{2\pi R_r R_t \cos\alpha}{\lambda D}\right)^2. \qquad (18)$$

Similar to the explanation for (17), the effect of $\cos\alpha$ is discounted much by D. The mathematical analysis in (17), (18) and the numerical results in Fig.2 indicates the effectiveness of the receive beam steering approach.

B. Off-axis and General Cases

In the off-axis case as shown in Fig.4, the transmit UCA and the receive UCA are parallel but not around the same axis. B is the distance of axis deviation. Through introducing a virtual UCA perpendicular to and in the middle of the connection between the transmit and the receive UCA centers, the off-axis case can be decomposed into two non-parallel cases: one from the transmit UCA to the virtual UCA, and the other from the virtual UCA to the receive UCA. Thus, the beam steering in the off-axis case needs both of the transmit UCA and the receive UCA steering their beams towards the virtual UCA.

Note that for the transmit UCA the azimuth and the elevation angle of the emergent OAM beam are $\pi/2$ and α respectively. So, the transmit beam steering vector $\mathbf{b}$ could be written as $\mathbf{b} = [1, e^{-jW'_2}, \cdots, e^{-jW'_N}]$, where

$$W'_n = \frac{2\pi R_t}{\lambda} \cos\left(\frac{2\pi(n-1)}{N} - \frac{\pi}{2}\right) \sin\alpha, \qquad (19)$$

$n = 1, \cdots, N$. Similarly, the ℓ-mode effective OAM channel with both the transmit and the receive beam steering can be formulated as

$$h''^{N}_{\text{eff}}(\ell) = \big(\mathbf{f}(\ell) \odot \mathbf{a}\big)\mathbf{H}\big(\mathbf{b}^T \odot \mathbf{f}^H(\ell)\big). \qquad (20)$$

Only in this way can the performance degradation caused by the off-axis misalignment be avoided to a large extent. Furthermore, from geometrical model we know that the more general misalignment cases could be solved by the combined use of the transmit and the receive beam steering as well.

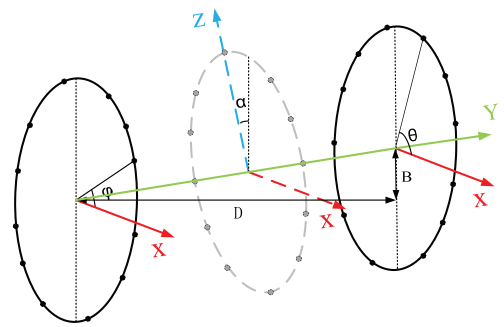

Fig. 4: The geometrical model of the transmit and the receive UCAs in the off-axis misalignment case.

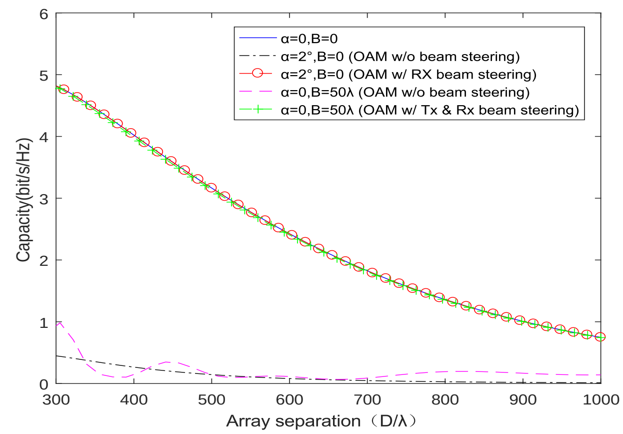

Fig. 5: The channel capacity comparison of the OAM without beam steering and the OAM with the proposed beam steering.

V. Numerical results

In this section, to verify the beam steering method, we simulate the UCA-based free space OAM communication system, in which the number of antenna elements of UCA N is equal to 12, the radius of the transmit UCA R_t and that of the receive UCA R_r are both equal to 10λ. The transmit SNR P_ℓ/σ_n^2 is assumed to be 30dB.

In Fig.5 we compare the capacity of the OAM channel without beam steering and the OAM channel with the proposed beam steering in non-parallel and off-axis cases. When there is the 2° oblique angle, the OAM channel capacity decreases to less than one tenth of its capacity in perfect alignment case. When there is an axis deviation, the OAM channel capacity also decays a large part and fluctuates with the distance of array separation. The reason of the fluctuation is that with the increase of array separation the fixed deviation distance results in the varying oblique angle for the transmit and receive beam steering. Fortunately, after applying the receive beam steering in the non-parallel case and both the transmit and the receive beam steering in the off-axis case, the misaligned OAM channel capacity is almost the same as that in perfect alignment case.

VI. Conclusion

In this paper, we investigate the effect of the misalignment between the transmit and the receive UCAs and the beam steering in the UCA-based free space OAM communication system. We show that the effective OAM channel gain and thus the OAM channel capacity drops rapidly as long as a very small oblique angle exists. To deal with the problem, we propose the transmit/receive beam steering approach to circumvent the large performance degradation in the non-parallel, the off-axis and other general misalignment cases, which paves the way for the application of OAM in practice.

References

[1] L. Allen, M. W. Beijersbergen, R. J. Spreeuw, and J. P. Woerdman, “Orbital angular momentum of light and the transformation of laguerre-gaussian laser modes,” *Physical Review A Atomic Molecular and Optical Physics*, vol. 45, no. 11, p. 8185, 1992.

[2] J. Wang, J. Y. Yang, and et al., “Terabit free-space data transmission employing orbital angular momentum multiplexing,” *Nature Photonics*, vol. 6, no. 7, pp. 488–496, 2012.

[3] M. Tamagnone, C. Craeye, and J. Perruisseaucarrier, “Encoding many channels on the same frequency through radio vorticity: first experimental test,” *New Journal of Physics*, vol. 14, no. 3, p. 033001, March 2013.

[4] B. Thid, H. Then, and et al., “Utilization of photon orbital angular momentum in the low-frequency radio domain.” *Physical Review Letters*, vol. 99, no. 8, p. 087701, 2009.

[5] Y. Yan, G. Xie, and et al., “High-capacity millimetre-wave communications with orbital angular momentum multiplexing,” *Nature Communications*, vol. 5, p. 4876, 2014.

[6] R. Gaffoglio, A. Cagliero, A. D. Vita, and B. Sacco, “OAM multiple transmission using uniform circular arrays: Numerical modeling and experimental verification with two digital television signals,” *Radio Science*, vol. 51, no. 6, pp. 645–658, 2016.

[7] G. Xie, L. Li, and et al., “Performance metrics and design parameters for a free-space communication link based on multiplexing of multiple orbital-angular-momentum beams,” *Physics*, pp. 481–486, 2014.

[8] Y. Zhang, W. Feng, and N. Ge, “On the restriction of utilizing orbital angular momentum in radio communications,” in *2013 8th International Conference on Communications and Networking in China (CHINACOM)*, Aug 2013, pp. 271–275.

[9] R. Chen, H. Xu, J. Li, and Y. Zhang, “Misalignment-robust receiving scheme for UCA-based OAM communication systems,” in *2017 IEEE 85th Vehicular Technology Conference (VTC2017-Spring)*, June 2017, pp. 1–5.

[10] W. Zhang, S. Zheng, X. Hui, R. Dong, X. Jin, H. Chi, and X. Zhang, “Mode division multiplexing communication using microwave orbital angular momentum: An experimental study,” *IEEE Trans. Wireless Commun.*, vol. 16, no. 2, pp. 1308–1318, Feb 2017.

[11] Y. Ren, L. Li, and et al., “Line-of-sight millimeter-wave communications using orbital angular momentum multiplexing combined with conventional spatial multiplexing,” *IEEE Trans. Wireless Commun.*, vol. PP, no. 99, pp. 3151–3161, 2017.

[12] G. Xie, Y. Yan, and et al., “Tunable generation and angular steering of a millimeter-wave orbital-angular-momentum beam using differential time delays in a circular antenna array,” in *2016 IEEE International Conference on Communications (ICC)*, May 2016, pp. 1–6.

[13] S. M. Mohammadi, L. K. S. Daldorff, J. E. S. Bergman, and R. L. Karlsson, “Orbital angular momentum in radio-a system study,” *IEEE Trans. Antennas Propag.*, vol. 58, no. 2, pp. 565–572, Feb 2010.

[14] F. E. Mahmouli and S. Walker, “Orbital angular momentum generation in a 60ghz wireless radio channel,” in *2012 20th Telecommunications Forum (TELFOR)*, Nov 2012, pp. 315–318.

[15] O. Edfors and A. J. Johansson, “Is orbital angular momentum (OAM) based radio communication an unexploited area?” *IEEE Trans. Antennas Propag.*, vol. 60, no. 2, pp. 1126–1131, 2012.

[16] W. L. Stutzman and G. A. Thiele, *Antenna theory and design*. Prentice-Hall, 1981.